Behavioral/Cognitive

Encoding and Representation of Intranasal CO_2 in the Mouse Olfactory Cortex

Kaitlin S. Carlson,* Christina Z. Xia,* and Daniel W. Wesson
Department of Neurosciences, Case Western Reserve University School of Medicine, Cleveland, Ohio 44106

Intranasal trigeminal sensory input, often perceived as a burning, tingling, or stinging sensation, is well known to affect odor perception. While both anatomical and functional imaging data suggest that the influence of trigeminal stimuli on odor information processing may occur within the olfactory cortex, direct electrophysiological evidence for the encoding of trigeminal information at this level of processing is unavailable. Here, in agreement with human functional imaging studies, we found that 26% of neurons in the mouse piriform cortex (PCX) display modulation in firing to carbon dioxide (CO_2), an odorless stimulant with known trigeminal capacity. Interestingly, CO_2 was represented within the PCX by distinct temporal dynamics, differing from those evoked by odor. Experiments with ascending concentrations of isopentyl acetate, an odorant known to elicit both olfactory and trigeminal sensations, resulted in morphing of the temporal dynamics of stimulus-evoked responses. Whereas low concentrations of odorant evoked responses upon stimulus onset, high concentrations of odorant and/or CO_2 often evoked responses structured to stimulus offset. These physiological experiments in mice suggest that PCX neurons possess the capacity to encode for stimulus modality (olfactory vs trigeminal) by differential patterns of firing. These data provide mechanistic insights into the influences of trigeminal information on odor processing and place constraints on models of olfactory-trigeminal sensory integration.

Introduction

Intranasal perception of airborne chemicals is mediated by both the olfactory and trigeminal systems. Indeed, while intranasal chemosensation is mostly attributed to olfaction, input from both of these sensory systems is critical for informing nutritional intake and avoidance of potentially harmful stimuli (Doty, 1995; Brand, 2006; Lundström et al., 2011). Major questions remain regarding the interaction of these systems in perceptually meaningful manners.

One reason why olfactory and trigeminal perceptual qualities are easily confused is that at high concentrations most odorants possess the capacity to elicit trigeminal sensations, which include intranasal burning, tingling, or prickling sensations (Doty et al., 1978, 1995). At low concentrations, however, most odorants fail to evoke trigeminal sensation. For example, nicotine is perceived to possess a musky odor at low concentrations, yet at high concentrations is a pungent nasal irritant (Edwards et al., 1987; Hummel and Kobal, 1992; Thuerauf et al., 1999). Further, the odorless trigeminal stimulant, carbon dioxide (CO_2), when presented with low-concentration odors, can impact pungency ratings of the odors (Cain and Murphy, 1980). Thus, there is considerable perceptual interplay between the olfactory and trigeminal systems that together result in our perception of odors (for review, see Brand, 2006).

The mechanisms whereby trigeminal sensation is encoded in the brain in manners capable of modulating olfaction remain unclear. Possibly subserving this, trigeminal sensory information converges into several olfactory structures (Yousem et al., 1997; Zald and Pardo, 2000; Billot et al., 2011; Lundström et al., 2011). There is direct anatomical innervation of the olfactory bulb by trigeminal fibers in the main olfactory epithelium (Schaefer et al., 2002). Trigeminal-evoked activity is observed within the olfactory epithelium (Tucker, 1971; Thürauf et al., 1991; Kratskin et al., 2000; Damann et al., 2006; Daiber et al., 2013) and the olfactory bulb (Hu et al., 2007; Gao et al., 2010). Human functional imaging studies have revealed that several structures display stimulus-dependent modulation in response to trigeminal stimulants, including the piriform cortex (PCX; Yousem et al., 1997; Zald and Pardo, 2000; Kollndorfer et al., 2013) and the olfactory tubercle (OT; Zelano et al., 2007). Related functional imaging studies have reported that even pure trigeminal stimulants, such as CO_2, evoke activity in the PCX (Hummel et al., 2009; Albrecht et al., 2010). This finding within the PCX, a structure considered critical for odor perception, including odor discrimination and odor learning (Haberly, 2001; Gottfried, 2010; Wilson and Sullivan, 2011), suggests nonolfactory sensory convergence in a manner that may underlie trigeminal influences on odor perception.

Some major questions remain, however, before being able to directly link trigeminal and olfactory physiological influences. At the most basic level, are CO_2 and other known trigeminal stimulants represented at the single-unit level in the olfactory cortex? If so, what are the spatial and temporal aspects of this

Received Jan. 28, 2013; revised July 12, 2013; accepted July 22, 2013.

Author contributions: K.S.C., C.Z.X., and D.W.W. designed research; K.S.C., C.Z.X., and D.W.W. performed research; K.S.C. and C.Z.X. analyzed data; K.S.C., C.Z.X., and D.W.W. wrote the paper.

This work was supported by National Science Foundation Grant IOS-1121471 to D.W.W. We are grateful for the comments of Dr. Thomas Hummel during the conception of this study and for helpful discussions with Dr. Vera Moiseenkova-Bell regarding interpretation of results.

*K.S.C. and C.Z.X. contributed equally to this work.

Correspondence should be addressed to Daniel Wesson, Department of Neurosciences, Case Western Reserve University School of Medicine, 2109 Adelbert Avenue, Cleveland, OH. E-mail: dww53@case.edu.

DOI:10.1523/JNEUROSCI.0422-13.2013

 0270-6474/13/3313873-09$15.00/0

encoding? Further, are concentration-dependent changes in trigeminal-elicited sensations also apparent among PCX neurons? To address these questions, here we performed *in vivo* electrophysiological multi- and single-unit recordings from anesthetized mice to explore the encoding and representation of trigeminal-evoked responses in the PCX. We focused our analyses mostly on activity elicited by CO_2, since this stimulus potently elicits trigeminal activity (Bensafi et al., 2008; Hummel et al., 2009; Wang et al., 2010; for review, see Luo et al., 2009), while sparing true olfactory sensation known to occur with numerous other trigeminal stimulants (e.g., ammonia, nicotine, menthol; Doty, 1995). Our results show that odor- and CO_2-evoked information converge onto a, respectively, large population of single units in the mouse olfactory cortex with distinct temporal dynamics that may underlie reports of olfactory-trigeminal integration.

Materials and Methods

Experimental subjects. Adult male C57BL/6 mice ($n = 27$, 2–4 months of age) were obtained from Harlan Laboratories and maintained within the Case Western Reserve University School of Medicine animal facility. Food and water were available *ad libitum*. The mice were on a 12 h light/dark cycle with all experiments performed during the light cycle. All experiments were conducted in accordance with the guidelines of the National Institutes of Health and were approved by the Case Western Reserve University's Institutional Animal Care Committee.

In vivo *electrophysiology.* Mice were anesthetized via urethane injection (1.0 mg/kg, i.p.) and mounted on a stereotaxic frame upon a water-filled heating pad (38°C). Anesthesia depth was verified by absence of toe-pinch reflex. A 0.05 ml injection of local anesthesia (1% lidocaine in 5% EtOH, s.c.) was then administered into the wound margin site before exposing the dorsal skull by removing the scalp. Two craniotomies were performed for electrode placement. First, a single hole was drilled from 0 mm anterior to bregma to 1.5 mm anterior to bregma for PCX and/or OT recording electrode placement. The second hole was drilled over the contralateral cortex to serve as entry for the reference electrode. Physiological (0.9%, 38°C) NaCl was applied to all craniotomy sites, which was replenished intermittently throughout the recording.

A tungsten electrode (0.01 in. o.d.; A-M Systems) was lowered into the reference craniotomy site ~1.5 mm deep. A second tungsten electrode (same type as above) was lowered into the PCX or OT and used as the recording electrode. The recording electrode activity was digitized at 28 kHz along with respiration and stimulus presentation events using a Tucker-Davis Technologies amplifier and software.

After recording, mice were transcardially perfused with 4°C 0.9% NaCl and then 10% formalin (Fisher Scientific). Following perfusion, the brains were removed and stored in 30% sucrose formalin at 4°C.

Electrode placement verification. All recording sites were verified by postmortem histological examinations of slide-mounted, 40 μm coronal brain sections stained with a 1% cresyl violet solution. PCX recording sites (layers i, ii, and/or iii; $n = 26$ from a total of 16 mice) were found across all coronal sections of the PCX (only the anterior regions of the PCX, containing the lateral olfactory tract, were used; Fig. 1). OT recording sites ($n = 17$ from a total of 11 mice) were found across all sections, but concentrated in the posterior area of the OT (layers i, ii, and/or iii; Fig. 1). Electrode tip locations were verified by multiple observers (K.C. and C.X.) with reference to a mouse brain atlas (Paxinos and Franklin, 2000).

Stimulus presentation. Filtered, ultrahigh purity medical grade CO_2 (AirGas) and/or odor (isopentyl acetate, 1 Torr dilution unless otherwise stated; Sigma Aldrich) were presented through a Teflon odor-port using a custom air-dilution olfactometer at the total flow rate of 1 L/min in all experiments. Stimuli were presented in a counterbalanced order, ≥4 trials/stimulus, at a ≥20 s interstimulus interval. The exit of the odor port was held at a distance of 1 cm from the tip of the nose. All stimulus lines were independent up to the point of immediate entry into the Teflon odor port, eliminating the potential of cross-stimulus contamination. In

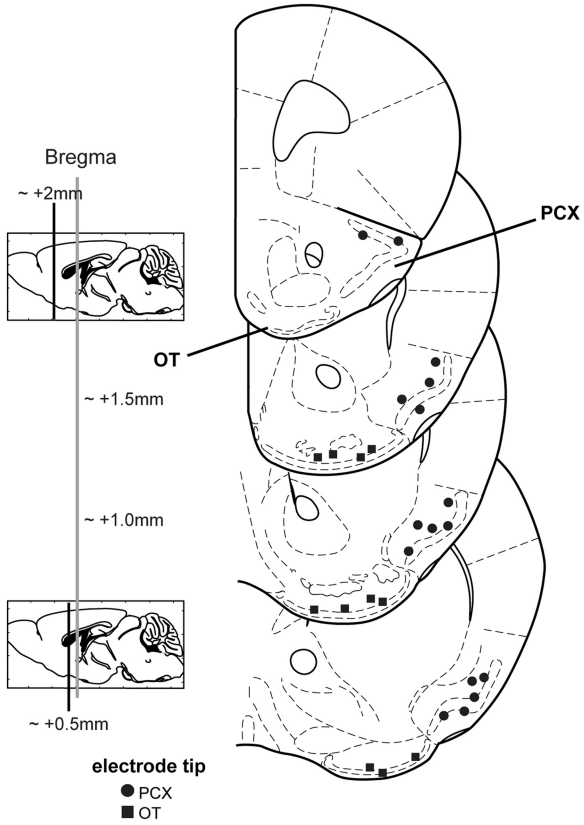

Figure 1. Electrode tip locations of PCX and OT recordings. Coronal stereotaxic panels showing the approximate location of the electrode tips following histological verification ($n = 16$ in PCX and 11 in OT). Total number of recording sites wherein units were collected and used for analysis = 26 in PCX and 17 in OT. Sections span from 2.0 to 0.5 mm anterior of bregma, in 0.5 mm intervals. Adapted from Paxinos and Franklin (2000).

all experiments, air dilution of CO_2 and odor were achieved using medical grade N_2. CO_2 stimuli (concentrations) arrived to the odor port by a single Teflon line wherein concentration of CO_2 (in N_2) was controlled between trials with an upstream flow controller. Stimulus onset (time to exit the odor port) was controlled across all stimuli by means of a vacuum line connected to a three-way solenoid valve. In our design, stimuli flowed toward and through the odor port for 20 s, in which time they were scavenged by the vacuum line. Computer-timed switching of the three-way solenoid valve resulted in a stimulus onset latency of <50 ms for all stimuli (measured with a piezo electric pressure-sensitive foil). Concentration of odor and CO_2 stimuli leaving the port were measured separately with a MiniRAE 3000 (used for odor; RAE Systems) and a TSI Q-Trak 7565 CO_2 meter. Measured values (averaged over 1 min, following application of instrument-specific correction factors) were 10 (odor), 3050 (50% CO_2), and 5820 ppm 100% CO_2. The 0% CO_2 (room air) was measured using the TSI Q-Trak at 450 ppm. Thus, this stimulus presentation paradigm resulted in dose-dependent concentrations of CO_2, all of which occurred within similar latencies. An analysis of respiration (via chest piezo sensor) from the present experiments failed to find an impact of CO_2 at either the 50% CO_2 ($F_{(1,12)} = 0.00004$, $p = 0.99$) or 100% CO_2 dilutions ($F_{(1,12)} = 0.038$, $p = 0.849$) on respiration rate (Fig. 2; 2 s prestimulus vs 2 s during stimulus, $n = 7$ mice, 8–12 trials/mouse).

The primary set of stimuli used to screen units for basic odor- and CO_2-evoked responses consisted of 50% CO_2, 100% CO_2, and odor (10% air [N_2] dilution of a 1 Torr liquid dilution) each at 2 s duration. In separate experiments, CO_2 and odor were each presented at four discrete concentrations (CO_2: 25, 50, 75, and 100%; odor: 1, 2, 3, and 4 Torr) to explore representation of these stimuli by units at varying concentrations. Following the recordings of the concentration data, in the same mice, we explored the temporal structure of unit responses to CO_2 by presenting 50% CO_2 for a duration of 2 and 4 s separately.

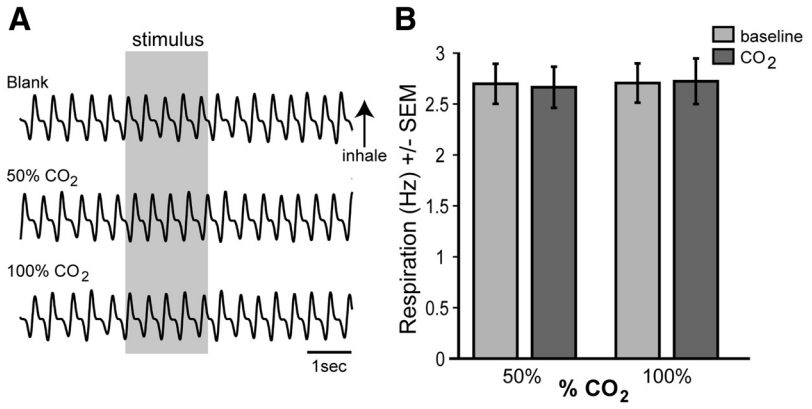

Figure 2. Respiratory frequency is independent of acute CO_2 presentation. ***A***, Example respiratory traces from an anesthetized mouse during presentation with "blank" (N_2), 50% CO_2, and 100% CO_2 stimuli (all at 1 L/min flow rate). ***B***, Mean respiratory frequency 2 s prior (baseline, −2 to 0 s) and during (0–2 s) presentation with either 50% or 100% CO_2. $n = 7$ mice, 8–12 trials/mouse.

Naris occlusion. Acute unilateral nasal occlusion was performed by applying odorless TorrSeal epoxy (Loctite; Westlake) on the naris ipsilateral to the recording hemisphere.

Data analysis. Waveform analysis and k-means cluster cutting were performed using Tucker-Davis Technologies software. Sorted data were verified to be independent units by an interspike interval analysis. For a unit to be considered a single unit, no more than 2% of all spikes could occur with an interspike interval < 2 ms. Putative single units that did not pass this criteria were omitted from further analysis.

The number of spikes (within 250 ms time bins) relative to the time of stimulus onset were extracted and organized by stimulus type. Custom macros written in Microsoft Excel were used to sort trials by stimulus type and calculate responsivity of neurons. A conservative p value ($p < 0.01$, two-tailed paired Student's t test) was used when comparing prestimulus (−2 to 0 s) to either during (0–2 s) or poststimulus epochs (2–4 s or 4–6 s) to identify stimulus-modulated units. These time epochs were selected after exploration of example traces to encompass both time periods in which we observed either odor-evoked (0–2 s, during stimulus) or CO_2-evoked activity (0–2, or 2–4 s after stimulus). For some analyses we calculated signal:noise ratios (s:n) as the average stimulus-evoked spike magnitude divided by the SD of the spontaneous firing (Payton et al., 2012; Varga and Wesson, 2013). This calculation differs from the standard ratio of stimulus-evoked spikes to all spikes, and was used to reduce variability in data due to trial-by-trial variability. Across region (OT vs PCX), stimuli (odor, 50% CO_2, 100% CO_2), and epoch (pre, during, post) comparisons were made using ANOVA followed by Fisher's PLSD. Statistical analyses were performed in Microsoft Excel or MATLAB (MathWorks). All data are reported as mean ± SEM unless otherwise noted.

Results

We sought to test whether single units in the PCX respond to a potent trigeminal stimulant, CO_2, and if so, to explore the nature of their stimulus-evoked dynamics. To initially address this, we recorded spontaneous and stimulus-evoked firing from cortical units in response to 50 and 100% CO_2 and a low concentration odor (isopentyl acetate). CO_2 was presented in a manner allowing its use as mostly a trigeminal (nonolfactory) stimulant (Hummel et al., 2009). Isopentyl acetate was selected due to its robust representation in both the PCX and OT (Payton et al., 2012). While this odorant is capable of eliciting trigeminal sensation at high concentrations (Doty et al., 1978, 1995; Porter et al., 2005), for our initial characterization of CO_2-evoked responses, we specifically used low concentrations of odor (~10 ppm; see Materials and Methods), allowing this to serve as a simple olfactory-evoked comparison. Additionally, all physiological recordings were performed from urethane-anesthetized mice to control for effects of behavioral state on unit firing (Kay and Laurent, 1999; Rinberg et al., 2006; Doucette and Restrepo, 2008) and respiration (Youngentob et al., 1987; Wesson et al., 2008; Fig. 2).

Robust representation of CO_2 among PCX neurons

In a first set of experiments, we recorded spontaneous and stimulus-evoked activity from 76 PCX neurons ($n = 9$ mice, 1–3 recording locations/mouse). We found that a substantial proportion of PCX units displayed robust modulations in firing in response to both odor and/or CO_2 (Fig. 3). As displayed in the example traces within Figure 3*A*, odor evoked a stereotypical increase in action potential firing upon stimulus onset, which decreased following stimulus offset. In contrast, this example unit displayed increased firing to 50% CO_2 upon stimulus offset, with no detectable firing during the stimulus. The 100% CO_2 failed to evoke firing in this unit, reflecting a level of concentration variance at least within this unit.

With the above example data demonstrating CO_2-evoked action potential firing among PCX units, we next sought to determine the population-level representation of CO_2 within this structure. Units were considered significantly modulated by comparing the number of spikes prestimulus (−2 to 0 s) to the number of spikes during or after stimulus presentation across all trials (0–2 s or 2–4 s) ($p < 0.01$, two-tailed, paired Student's t test). A significant p value to either time bin comparison (0–2 s or 2–4 s) was used as an indicator of a modulated unit to not bias designation as modulated based upon temporal dynamics. These time epochs were selected after careful exploration of example traces to encompass both time periods during which we regularly observed either odor (0–2 s, during stimulus) or CO_2-evoked activity (2–4 s, after stimulus, see Fig. 3*A*).

We found that 26.3% of PCX units were modulated by at least one of the CO_2 stimuli (20/76; Fig. 3*B*). The majority (17.1%, 13/76) of CO_2-modulated neurons in the PCX were CO_2 selective, failing to also show modulation in response to odor. Of these CO_2-selective neurons, 46.2% (6/13) were modulated by 50% CO_2 and 53.8% (7/13) were modulated by 100% CO_2, reflecting similar representation of these concentrations at the population level (χ^2 (1) = 0.154, $p = 0.695$; Fig. 3*B*). While a modest number, 9.2% (7/76) of CO_2-modulated neurons were bimodal, displaying significant modulation to both CO_2 and the low-concentration odor, reflecting convergence at the single neuron level of odor- and CO_2-evoked information within the PCX.

Temporal dynamics of CO_2-evoked responses in the PCX

The example traces shown in Figure 3*A* suggest that CO_2 is represented among PCX neurons at a different time course than odor. We sought to quantify this by creating peristimulus histograms of the mean number of spikes (within 250 ms time bins) from all PCX neurons in response to each three stimuli ($n = 9$ mice, 76 units). As suggested by the traces in Figure 3*A*, a peristimulus plot containing only data from neurons modulated by each stimulus category supports these unique differences in temporal dynamics between odor and CO_2, with both 50 and 100%

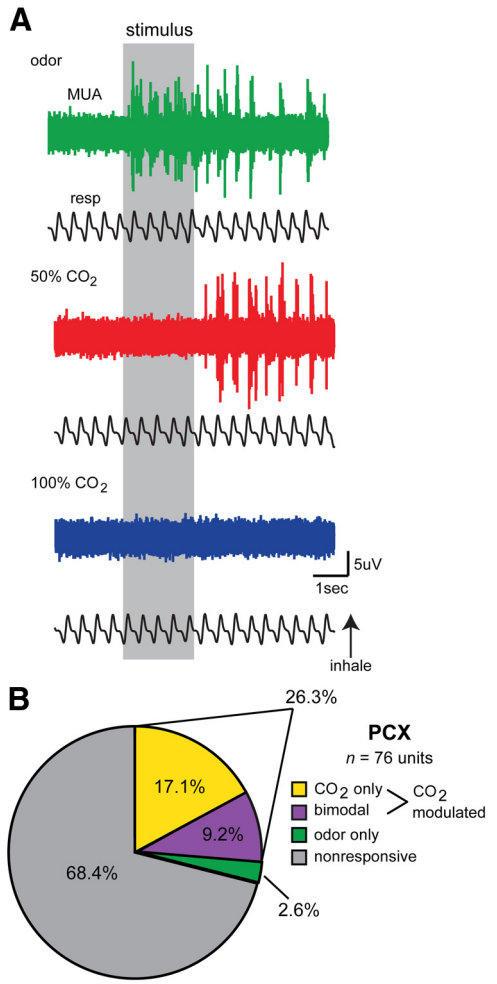

Figure 3. Characteristics of CO_2-evoked activity in the PCX. ***A***, Representative traces of multi-unit activity (MUA) from a single PCX recording during presentation with odor (isopentyl acetate), 50% CO_2, and 100% CO_2. In this example, MUA (spiking) increases during presentation with odor (isopentyl acetate), which decays following odor offset. In contrast, presentation of 50% CO_2 elicits increased spiking only after stimulus offset, which in this example is not also displayed in response to 100% CO_2. This MUA reflects a (or several) bimodal unit that responds to both odor and CO_2. ***B***, PCX single-unit response distribution pie chart organized by significant stimulus type ($p < 0.01$, two-tailed paired *t* tests, total # of spikes −2 to 0 s vs 0–2 s) ($n = 11$ mice, 1–3 recording sites/mouse). Single units were considered CO_2 modulated if they were selective in responding to only with 50% or 100% CO_2, or if they responded to either 50% or 100% CO_2 and odor (isopentyl acetate); 68.4% of units failed to display stimulus-modulated activity ($p > 0.01$, two-tailed paired *t* tests).

CO_2-evoked responses reaching peak magnitude ~1 s post stimulus offset, ~2 s following the peak in odor-evoked activity (Fig. 4*A*). These dynamics were displayed differentially by each neuron in the population, with detectable changes in firing during stimulus mostly observed only in response to odor (Fig. 4*B*).

Quantitative comparisons of mean unit firing among only significantly modulated neurons revealed that significant changes in firing during the stimulus epoch were only observed for odor ($F_{(1,16)} = 8.275$, $p = 0.011$; pre vs during; Fig. 4*C*). Following stimulus offset, both 50 and 100% CO_2 evoked significant increases in firing compared with both spontaneous (50% $F_{(1,24)} = 28.103$, $p < 0.0001$; 100% $F_{(1,16)} = 9.076$, $p = 0.0083$) and during stimulus epochs (50% $F_{(1,24)} = 22.92$, $p < 0.0001$; 100% $F_{(1,16)} = 4.925$, $p = 0.041$; Fig. 4*C*). Interestingly, within their respective modulatory time points (during stimulus for odor and post for CO_2), both 50% ($F_{(1,20)} = 0.008$, $p = 0.93$) and 100% CO_2 ($F_{(1,16)} = 0.166$, $p = 0.69$) evoked similar amounts of spiking compared with odor. These results demonstrate that CO_2 is represented among PCX single units by unique temporal dynamics compared with odor.

Inverse relationship between odor and CO_2 intensity on PCX unit responses

Several questions are raised based upon these initial observations. First, as suggested by the surprisingly similar responses of modulated units to 50 and 100% CO_2 (Fig. 4), do PCX units as a population display concentration variance of CO_2 sensory input? Related, and second, are the unique temporal dynamics observed in response to CO_2 a specific characteristic of CO_2-evoked activity at this level, or a more general activity pattern that could be similarly evoked by other trigeminal stimulants?

To address these questions, we recorded PCX unit activity in a separate cohort of animals ($n = 7$ mice) throughout exposure to a concentration series of both CO_2 (25, 50, 75, and 100%) and odor (1, 2, 3, and 4 Torr). Histograms of s:n responses (see Materials and Methods) to odor and CO_2 from three example units are displayed in Figure 5*A*. These example units reflect an inverse relationship between odor and CO_2 encoding at the level of PCX units, in terms of their responses during, compared with after, stimulus. In one dramatic example (Fig. 5*A*, far left) CO_2 is represented by increased s:n following but not during stimulus duration, up to the point that the concentration of the CO_2 reaches 100%, at which time the large offset response characteristic of 25–75% CO_2 disappears. In contrast, this unit represents increasing concentrations of odor with increasing s:n during the stimulus, which at highest concentrations (4 Torr) is also accompanied with a respectfully large offset response. This increased offset response for 4 Torr odor resembles offset responses observed to CO_2, and is not displayed by every unit (Fig. 5*A*, far right), suggesting this is not an artifact of failure for the nose to clear odor at this concentration. Interestingly, some units (Fig. 5*A*, middle) failed to display major increases in s:n for the 4 Torr odor, instead displaying a substantially greater s:n during offset in these presentations (Fig. 5*B*). Results across all spontaneously active units ($n = 18$), displayed in Figure 5*C*, reflect that as a population, PCX units represent odor and CO_2 in temporally divergent manners, yet at qualitatively similar magnitudes depending upon the time epoch (during vs poststimulus). The overall profile of responses across all concentrations results in an inverted U-shape distribution during odor onset, but contrastingly, during offset for CO_2. This effect is summarized in Figure 5*D*, and demonstrates that (1) PCX units as a population represent CO_2 in a concentration variant fashion and (2) offset responses among PCX units appear as a generalized response property of these cells to putative trigeminal stimuli as a stimulus class, not just CO_2.

CO_2-evoked PCX unit activity requires inhalation

While the example traces in Figure 3 suggest that PCX unit firing in response to CO_2 displays respiratory coupling, it is also possible that CO_2-evoked activity is entering the PCX following transduction by a variety of putative CO_2-sensitive channels or receptors on the eyes, face, and/or mouth (Guimaraes and Jordt, 2007; Gerhold and Bautista, 2009). To directly test whether inhalation of CO_2 is required for CO_2-evoked PCX unit firing, we took advantage of the fact that mice are obligate nasal-air breathers and performed ipsilateral naris occlusion during the course of recording multi-unit activity in response to 50% CO_2 ($n = 7$ mice, same as used in Fig. 5). As shown in the example traces in Figure 6*A*, stimulus-offset multi-unit (and also local field poten-

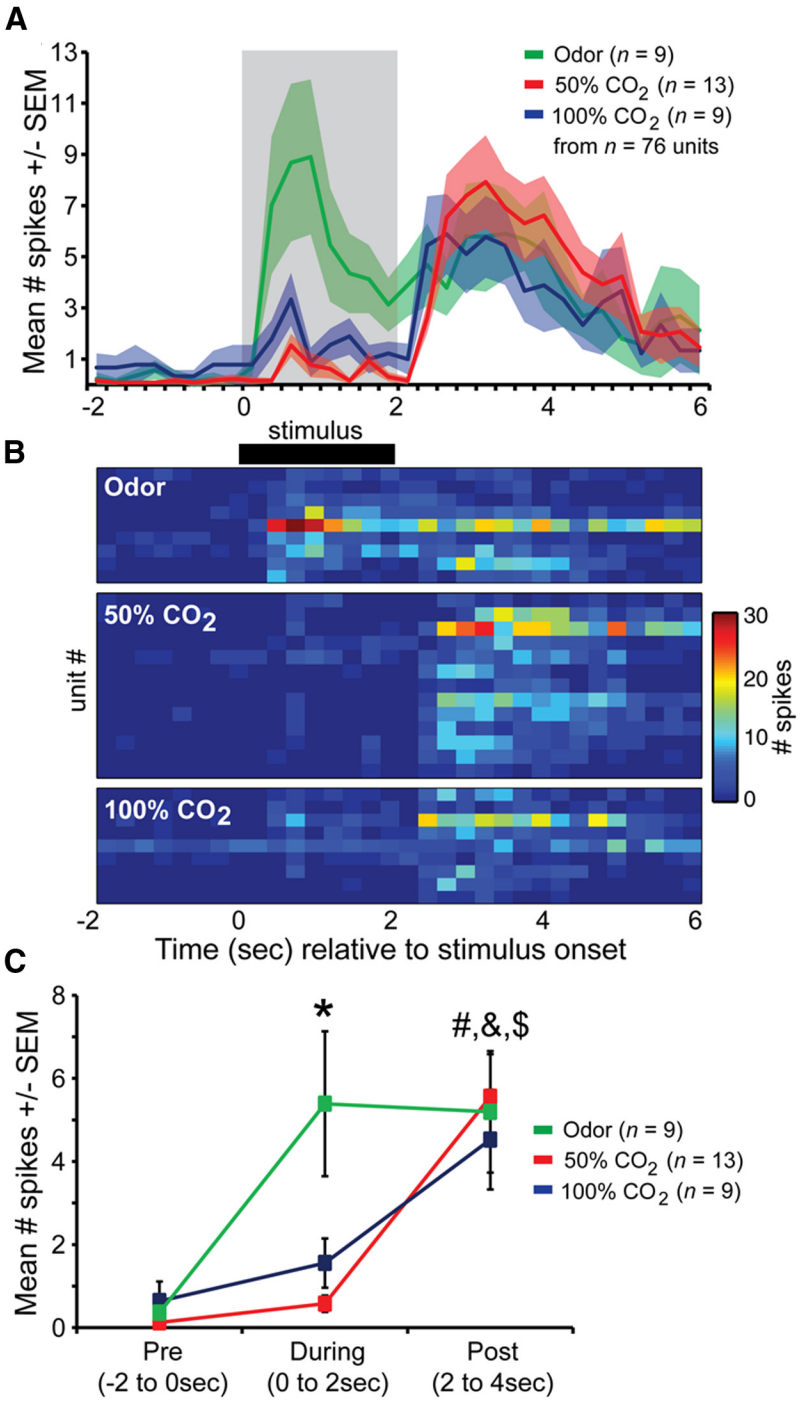

Figure 4. Distinct timescale of CO_2-evoked PCX single-unit activity. ***A***, Average spike number across all PCX units significantly modulated ($p < 0.01$) by odor (isopentyl acetate), 50% CO_2, and 100% CO_2. Gray shaded box = stimulus duration. $n = 76$ units total in screen. ***B***, 2D histogram displaying spiking of individual single units (same data as in ***A***). ***C***, Mean spike # across all modulated units (same as in ***A*** and ***B***) prestimulus ("Pre," −2 to 0 s), during stimulus (0–2 s), or poststimulus ("Post," 2–4 s). $^{*}p < 0.05$, pre versus during (odor). $^{\#}p < 0.01$, pre versus post (50 and 100% CO_2). $^{\&}p < 0.0001$ (50% CO_2), $^{\$}p < 0.05$ (100% CO_2), during versus post. All statistics are ANOVA followed by Fisher's PLSD.

tial) responses to 50% CO_2 were abolished with ipsilateral naris occlusion. Quantification of CO_2-evoked spiking across all mice ($n = 15$ units) revealed that naris occlusion significantly decreases spiking during stimulus-offset compared with the activity previously elicited by CO_2 while the naris was open (Fig. 6*B*; $F_{(1,24)} = 18.236$, $p = 0.0003$). These results demonstrate that in this context, CO_2-evoked activity enters the PCX following intranasal inhalation/transduction.

Distribution of CO_2-evoked responses in the olfactory cortex

Is the PCX uniquely involved in representing trigeminal information at this level of processing? To explore this question, we performed additional recordings of stimulus-evoked responses from neurons in the neighboring OT ($n = 11$ mice, 57 units, 1–3 recording locations/mouse). Similar to the PCX, the OT receives dense olfactory sensory input from mitral and tufted cells in the olfactory bulb, but also other sensory information from association structures (Wesson and Wilson, 2011). We found that only 3.5% (2/57) of OT units were modulated by CO_2 (Fig. 7; 1–50% CO_2, 1–100% CO_2). Among the two CO_2-modulated units, none were bimodal in responding significantly to both odor and CO_2. The PCX possessed a significantly greater number of CO_2-modulated neurons compared with the OT ($\chi^2(1) = 10.676$, $p = 0.0011$; Fig. 7). Thus, at the population level, the PCX plays a unique role in the representation and processing of intranasal trigeminal information compared with the OT.

CO_2-evoked responses are structured to stimulus offset

CO_2-sensitive PCX neurons appear to structure their response excitation based upon CO_2 stimulus offset. To test if indeed CO_2-responsive neuronal responses are structured to stimulus offset, we performed additional experiments ($n = 7$ mice, same as used for Fig. 5) wherein we presented 50% CO_2 for either 2 s or 4 s durations. We later compared the latency to peak firing among PCX single units relative to stimulus onset between the 2 s CO_2 and 4 s CO_2 conditions (only from neurons displaying significant modulation during stimulus offset, $n = 19$ [2 s], $n = 17$ [4 s]). As shown in Figure 8, across all significantly modulated (excitatory) units in both stimulus conditions, spiking did not increase until following CO_2 offset. At the individual unit levels, the probability of a single unit reaching maximum firing (spike # within 250 ms time bin) increased dramatically post, yet not before, stimulus offset (Fig. 8*B*). These data demonstrate that CO_2-evoked dynamics are shaped by the duration of CO_2 stimulation in a manner that might impact the temporal interaction between odor-evoked and trigeminal-evoked information at this level.

Discussion

Trigeminal sensation, including the burning and tingling sensations elicited by intranasal CO_2 and high-concentration odorants, are well known to modulate olfactory perception (Cain and

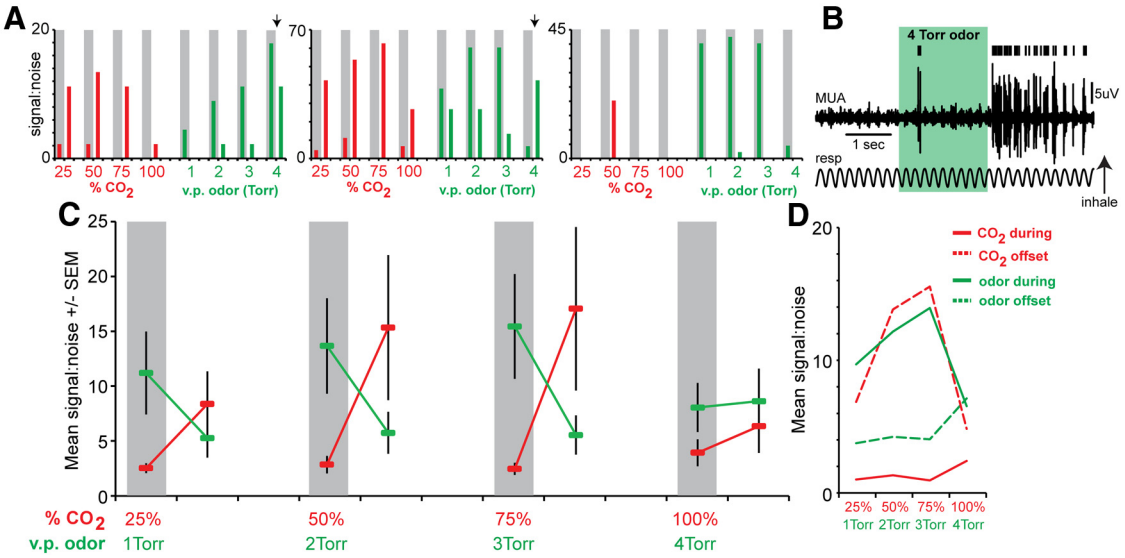

Figure 5. Inverse relationship between odor and CO_2 intensity on PCX unit responses. ***A***, S:n histograms of three example PCX units throughout concentration series of both odor (isopentyl acetate) and CO_2. Gray shaded bar = 0–2 s during stimulus. Unshaded epoch after stimulus epos = 2–4 s post stimulus. The first two example units displayed increased offset firing to a high concentration of odor (vertical downward arrow), which was not present at low concentrations of odor nor was it displayed by the third example unit. The third example unit reflects a case wherein the most potent odor stimulus failed to evoke a response comparable to the previous three (weaker) odor conditions. v.p., Vapor pressure. ***B***, Example trace from middle unit shown in ***B*** in response to a single trial of 4 Torr odor. ***C***, Mean s:n across all units ($n = 18$ spontaneously active units, 7 mice) to ascending concentrations of odor and CO_2. ***D***, Same data as in ***C***, but arranged within stimulus types, by "during" and "offset" epochs. These data reflect that PCX units represent increasing concentrations of odor in similar manners as increasing intensity of CO_2, but with highly different temporal dynamics (CO_2-evoked changes occurring poststimulation). MUA, multi-unit activity.

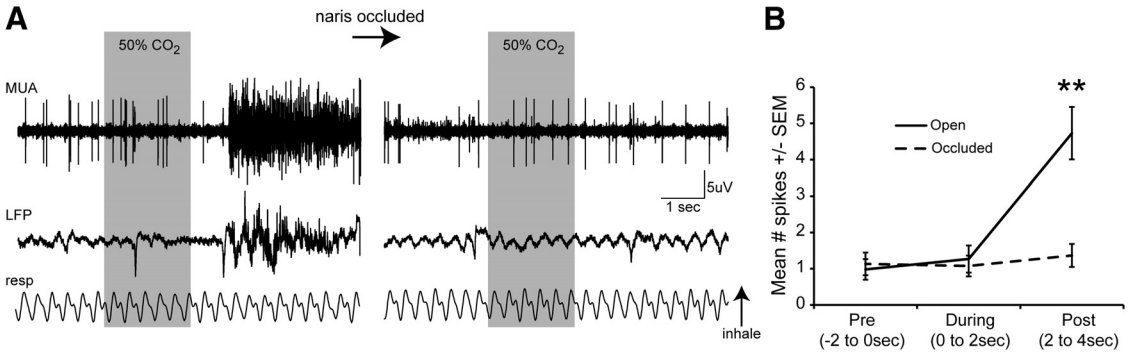

Figure 6. Ipsilateral naris occlusion abolishes CO_2-evoked excitation. ***A***, Multi-unit activity (MUA), local field potential (LFP; 0—100 Hz second-order bandpass filter), and respiration traces displaying activity of a CO_2-modulated unit during presentation with 50% CO_2 before (left) and ~1 min after (right) ipsilateral naris occlusion (see Materials and Methods). ***B***, Mean spike # across units prestimulus (Pre, −2 to 0 s), during stimulus (0–2 s), or poststimulus (Post, 2–4 s), both before naris occlusion ("open") and after ("occluded"). The occlusion was not reversible, thus each animal contributed only 1 trial/condition. $n = 7$ mice. $^{**}p < 0.001$, open versus occluded, ANOVA followed by Fisher's PLSD.

Murphy, 1980; Silver and Finger, 1991; Doty, 1995; Brand, 2006). In the present studies we used two separate stimulants with known trigeminal capacity: CO_2 and high-concentration isopentyl acetate. While both stimuli are capable of stimulating the trigeminal system, it is important to clarify that neither are entirely selective (Doty, 1995; Luo et al., 2009). Nevertheless, our findings provide direct electrophysiological evidence for intranasal CO_2-evoked responses at the single-unit level within the olfactory cortex. These responses were observed among 26.3% of PCX single units and at statistically greater amounts than observed in the neighboring OT. A considerably small subset of PCX single units displayed multimodal convergence of CO_2 and a low concentration odor. The present results build upon and extend previous functional imaging studies demonstrating the presence of CO_2-evoked responses in the PCX (Hummel et al., 2009; Albrecht et al., 2010; Bensafi et al., 2012) and provide physiological evidence that the known perceptual interplay between odor and trigeminal stimuli (Doty et al., 1978, 1995; Cain and Murphy, 1980; Livermore and Laing, 1996; Brand, 2006; Boesveldt et al., 2007; Bensafi et al., 2008; Kleemann et al., 2009; Wise et al., 2012) may occur at the level of the single neuron within the olfactory cortex.

Unique spatial and temporal representation of CO_2 in the olfactory cortex

Here we found that CO_2 elicited increases in neural activity largely within the PCX. This robust level of activity evoked by CO_2 in the PCX, but not the OT, perhaps underlies reports of CO_2-evoked activity in human PCX (Albrecht et al., 2010). In contrast, similar inter-regional differences were not found in response to odor (Fig. 7; Payton et al., 2012). This striking, and significant difference in the recruitment of olfactory cortex neurons by CO_2 stimulation suggests major inter-regional differences in the processing of CO_2. This finding further suggests fundamental differences in anatomical innervation of these two structures by CO_2-sensitive neurons, or by neurons that receive synaptic input from CO_2-sensitive neurons.

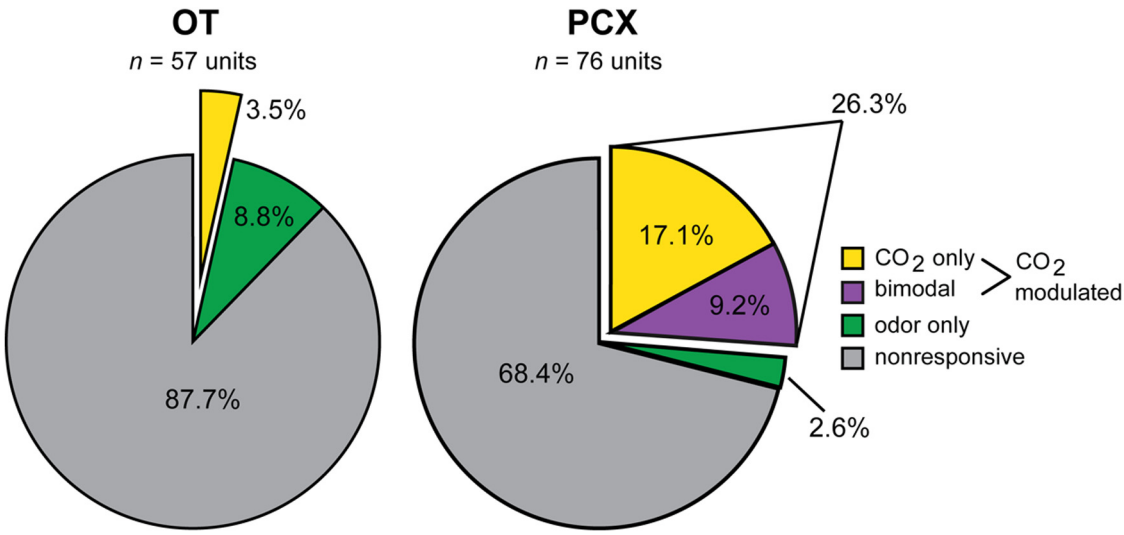

Figure 7. Representation of CO_2-evoked activity throughout the olfactory cortex. OT (left) single-unit response distribution pie chart organized by significant stimulus type ($p < 0.01$, two-tailed paired *t* tests, total # of spikes −2 to 0 s vs 0–2 s). Single units were considered CO_2 modulated if they were selective in responding to only 50% or 100% CO_2, or if they responded to either 50% or 100% CO_2 and odor (isopentyl acetate). Also displayed for comparison purposes is the PCX single-unit response distribution (right, same as in Fig. 3*B*). Whereas 28.9% of PCX units were CO_2 modulated, only 3.5% of those in the OT were. No bimodal neurons were found within the OT.

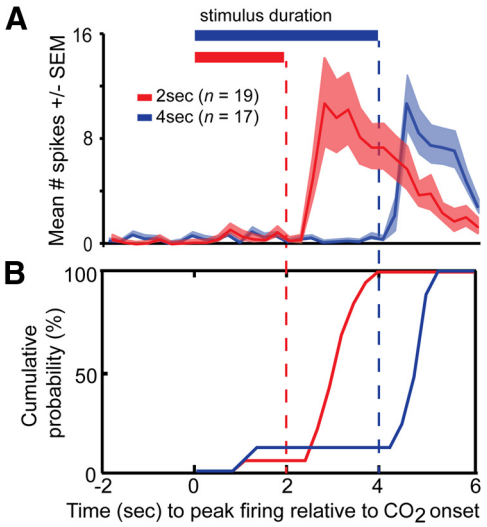

Figure 8. CO_2-evoked responses are structured to stimulus offset. ***A***, Average spike number across PCX units significantly modulated ($p < 0.05$, pre vs offset) in response to 2 s 50% CO_2 (red; $n = 19$ units) or 4 s 50% CO_2 (blue; $n = 17$ units). Horizontal bars = duration of CO_2. Vertical dashed lines = stimulus offset. $n = 7$ mice. ***B***, Cumulative distribution comparing the latency of CO_2-modulated (excitatory) unit responses to 2 and 4 s stimuli (same as in ***A***). Latency = time from stimulus onset to 250 ms bin with peak number of spikes. The majority (>85%) of single units do not reach peak firing until stimulus offset in both 2 and 4 s conditions.

CO_2-evoked responses in the PCX consisted of delayed transient dynamics–with little to no increases in excitatory firing displayed during stimulus presentation. Instead, the bulk of stimulus-evoked firing occurred following stimulus offset. The temporal dynamics of these putatively trigeminal-mediated patterns of PCX firing are the direct opposite of most odorant-evoked firing observed within the olfactory cortex. Classically, odorant-evoked responses in the olfactory cortex occur upon the first inhalation of odorant (Fig. 3) (Schoenbaum and Eichenbaum, 1995; Wilson, 2000; Rennaker et al., 2007; Chapuis and Wilson, 2011; Payton et al., 2012; Rampin et al., 2012). Some examples, however, of delayed excitatory responses to odorants among PCX neurons are present (Rennaker et al., 2007) perhaps reflecting that at their respectfully strong concentrations used, these odorants possessed a trigeminal component (Doty et al., 1978). In contrast, here we used a considerably low concentration of a single odorant, isopentyl acetate, known at higher concentrations to recruit a large portion of OT and PCX neurons (Payton et al., 2012), though at the concentration used herein recruited considerably less units (albeit while sparing likely trigeminal responsivity, as suggested by a significantly reduced representation of odor vs CO_2 in both structures (Fig. 7). Interestingly, upon increasing the concentration of this odorant, we showed that the temporal dynamics of stimulus-evoked firing in some PCX neurons can be altered from showing onset (low-concentration odorant) to offset responses (high-concentration odorant) (Fig. 5). Thus, based upon these data it is highly likely that single neurons possess the capacity to encode for stimulus modality (olfactory vs trigeminal) by differential patterns of firing (onset vs offset).

Based upon the present findings, an important goal for future research will be to identify the mechanisms for the delayed response onset for CO_2 observed among PCX neurons. The substantial differences in latency to spiking between odor and CO_2 suggests the stimulus-evoked information from these two stimuli enters the PCX by means of distinct routes or quite possibly by distinct biochemical transduction elements. Regarding the latter, the transduction of CO_2 upon nasal inhalation may occur by TRPA1 channels on trigeminal ganglia (Guimaraes and Jordt, 2007; Wang et al., 2010). TRPA1 is activated by CO_2 via the gating of intracellular protons (Wang et al., 2011). CO_2 is known to specifically activate a subset of trigeminal neurons in a manner dependent upon *TRPA1* gene expression (Wang et al., 2010). In mice, CO_2 transduction may also be mediated by specialized olfactory sensory neurons within the nasal cavity that express guanylyl cyclase D (Hu et al., 2007), which is also being largely regulated by extracellular or intracellular pH that is tightly controlled by CO_2 delivery (Luo et al., 2009). Indeed, nasal pH decreases with CO_2 stimulation (Shusterman and Avila, 2003), following which, offset of the CO_2 stimulus would allow pH levels to rebound and thereby possibly increase the spiking of specific neurons through altered transduction rates. The neural mecha-

nisms of CO_2 sensing have received considerable recent attention in both vertebrates and invertebrates (Hu et al., 2007; Luo et al., 2009; Turner and Ray, 2009; Wang et al., 2011) and future work addressing this question at the level of the PCX will be highly informative in translating this work into a better understanding of possible olfactory-trigeminal integration.

Trigeminal-olfactory multisensory convergence in the olfactory cortex

While only using a single odorant, and thereby limiting the absolute understanding of bimodal convergence in this structure, our finding that CO_2- and odor-evoked information converges at the single-unit level in the mouse olfactory cortex adds to a growing body of literature regarding the role of the olfactory cortex in multisensory integration. PCX single units in rodents display both gustatory-evoked (Maier et al., 2012) and auditory-evoked activity (Varga and Wesson, 2013). Further, PCX activity is modulated by visual sensory-input in humans (Gottfried and Dolan, 2003), in a manner that even modulates olfactory perception (Gottfried and Dolan, 2003; Jadauji et al., 2012). In addition to the PCX, the OT also displays olfactory-auditory sensory convergence (Wesson and Wilson, 2010). Thus, together, these results reflect that the olfactory cortex, particularly the PCX and OT, do not serve as only unimodal olfactory processing centers, but in fact are polysensory structures. Indeed, other primary sensory cortices, including those of audition and vision, are also increasingly becoming understood to integrate multisensory information in manners that may underlie the enhancement of perception and behavior in polysensory contexts (Foxe et al., 2002; Schroeder and Foxe, 2005; Ghazanfar and Schroeder, 2006; Kayser and Logothetis, 2007; Lakatos et al., 2007; Cohen et al., 2011; Iurilli et al., 2012). Future studies exploring the principles of trigeminal-olfactory convergence as reported herein will be informative in elucidating neural mechanisms underlying the modulation of odor perception by trigeminal stimuli. This will be largely made possible by using additional stimuli with known trigeminal properties (nicotine, ammonia, etc.) in behaving animals in combination with physiological recordings.

Implications of convergence within the cortex on perception

The considerably large representation of CO_2-evoked responses in the PCX, and particularly the convergence of trigeminal (CO_2 and high concentration odorant) sensory information onto single "bimodal" units within the PCX, suggests a likely major influence of trigeminal information on the processing of odors in the PCX. At the most basic level, these results support the impact of trigeminal sensory input on odor processing within the cortex. The PCX (Gottfried, 2010; Wilson and Sullivan, 2011) and OT (Wesson and Wilson, 2011) are both hypothesized as critical for olfactory perception. Thus, disruption of normal odor coding by single neurons within these structures by incoming trigeminal-evoked neural activity would impact odor learning and odor perception. Indeed, CO_2 alters odor perception in humans (Cain and Murphy, 1980; Kleemann et al., 2009; Daiber et al., 2013). Relatedly, based upon the present findings that the bulk of CO_2-evoked activity initiated upon stimulus offset, we predict that the critical window for trigeminal sensory input to impact the processing of odors in the PCX would occur following the immediate inspiration of the odor. In this case, trigeminal stimulation might affect the lingering, persistent sensation of odors and consequently reporting of odor perceptual qualities–throughout which the entire time somatosensory components of the trigeminal stimuli (burning, tingling) are being perceived likely through impact on somatosensory cortex (Hummel et al., 2009). This differs from the common assumption that for these stimuli to have cross-modal associations, they would likely modulate activity among single neurons simultaneously. Tests of this prediction with experiments to modulate the precise timing of odor inhalations as they relate to CO_2 delivery could provide insights into this question and further our understanding of mechanisms whereby trigeminal information may modulate odor perception.

References

Albrecht J, Kopietz R, Frasnelli J, Wiesmann M, Hummel T, Lundström JN (2010) The neuronal correlates of intranasal trigeminal function—an ALE meta-analysis of human functional brain imaging data. Brain Res Rev 62:183–196. CrossRef Medline

Bensafi M, Iannilli E, Gerber J, Hummel T (2008) Neural coding of stimulus concentration in the human olfactory and intranasal trigeminal systems. Neuroscience 154:832–838. CrossRef Medline

Bensafi M, Iannilli E, Poncelet J, Seo HS, Gerber J, Rouby C, Hummel T (2012) Dissociated representations of pleasant and unpleasant olfactotrigeminal mixtures: an fMRI study. PLoS One 7:e38358. CrossRef Medline

Billot PE, Comte A, Galliot E, Andrieu P, Bonnans V, Tatu L, Gharbi T, Moulin T, Millot JL (2011) Time course of odorant- and trigeminal-induced activation in the human brain: an event-related functional magnetic resonance imaging study. Neuroscience 189:370–376. CrossRef Medline

Boesveldt S, Haehner A, Berendse HW, Hummel T (2007) Signal-to-noise ratio of chemosensory event-related potentials. Clin Neurophysiol 118:690–695. CrossRef Medline

Brand G (2006) Olfactory/trigeminal interactions in nasal chemoreception. Neurosci Biobehav Rev 30:908–917. CrossRef Medline

Cain WS, Murphy CL (1980) Interaction between chemoreceptive modalities of odor and irritation. Nature 284:255–257. CrossRef Medline

Chapuis J, Wilson DA (2011) Bidirectional plasticity of cortical pattern recognition and behavioral sensory acuity. Nat Neurosci 15:155–161. CrossRef Medline

Cohen L, Rothschild G, Mizrahi A (2011) Multisensory integration of natural odors and sounds in the auditory cortex. Neuron 72:357–369. CrossRef Medline

Daiber P, Genovese F, Schriever VA, Hummel T, Möhrlen F, Frings S (2013) Neuropeptide receptors provide a signalling pathway for trigeminal modulation of olfactory transduction. Eur J Neurosci 37:572–582. CrossRef Medline

Damann N, Rothermel M, Klupp BG, Mettenleiter TC, Hatt H, Wetzel CH (2006) Chemosensory properties of murine nasal and cutaneous trigeminal neurons identified by viral tracing. BMC Neurosci 7:46. CrossRef Medline

Doty RL (Ed.) (1995) Intranasal trigeminal chemoreception anatomy, physiology, and psychophysics. In: Handbook of olfaction and gustation, pp 821–833. New York: Marcel Dekker.

Doty RL, Brugger WE, Jurs PC, Orndorff MA, Snyder PJ, Lowry LD (1978) Intranasal trigeminal stimulation from odorous volatiles: psychometric responses from anosmic and normal humans. Physiol Behav 20:175–185. CrossRef Medline

Doucette W, Restrepo D (2008) Profound context-dependent plasticity of mitral cell responses in olfactory bulb. PLoS Biol 6:e258. CrossRef Medline

Edwards DA, Mather RA, Shirley SG, Dodd GH (1987) Evidence for an olfactory receptor which responds to nicotine–nicotine as an odorant. Experientia 43:868–873. CrossRef Medline

Foxe JJ, Wylie GR, Martinez A, Schroeder CE, Javitt DC, Guilfoyle D, Ritter W, Murray MM (2002) Auditory-somatosensory multisensory processing in auditory association cortex: an fMRI study. J Neurophysiol 88:540–543. Medline

Gao L, Hu J, Zhong C, Luo M (2010) Integration of CO2 and odorant signals in the mouse olfactory bulb. Neuroscience 170:881–892. CrossRef Medline

Gerhold KA, Bautista DM (2009) Molecular and cellular mechanisms of trigeminal chemosensation. Ann NY Acad Sci 1170:184–189. CrossRef Medline

Ghazanfar AA, Schroeder CE (2006) Is neocortex essentially multisensory? Trends Cogn Sci 10:278–285. CrossRef Medline

Gottfried JA (2010) Central mechanisms of odour object perception. Nat Rev Neurosci 11:628–641. CrossRef Medline

Gottfried JA, Dolan RJ (2003) The nose smells what the eye sees: crossmodal visual facilitation of human olfactory perception. Neuron 39:375–386. CrossRef Medline

Guimaraes MZP, Jordt SE (2007) TRPA1: a sensory channel of many talents. In: TRP ion channel function in sensory transduction and cellular signaling cascades (Liedtke WB, Heller S, eds). Boca Raton, FL: CRC.

Haberly LB (2001) Parallel-distributed processing in olfactory cortex: new insights from morphological and physiological analysis of neuronal circuitry. Chem Senses 26:551–576. CrossRef Medline

Hu J, Zhong C, Ding C, Chi Q, Walz A, Mombaerts P, Matsunami H, Luo M (2007) Detection of near-atmospheric concentrations of CO2 by an olfactory subsystem in the mouse. Science 317:953–957. CrossRef Medline

Hummel T, Kobal G (1992) Differences in human evoked potentials related to olfactory or trigeminal chemosensory activation. Electroencephalogr Clin Neurophysiol 84:84–89. CrossRef Medline

Hummel T, Oehme L, van den Hoff J, Gerber J, Heinke M, Boyle JA, Beuthien-Baumann B (2009) PET-based investigation of cerebral activation following intranasal trigeminal stimulation. Hum Brain Mapp 30:1100–1104. CrossRef Medline

Iurilli G, Ghezzi D, Olcese U, Lassi G, Nazzaro C, Tonini R, Tucci V, Benfenati F, Medini P (2012) Sound-driven synaptic inhibition in primary visual cortex. Neuron 73:814–828. CrossRef Medline

Jadauji JB, Djordjevic J, Lundström JN, Pack CC (2012) Modulation of olfactory perception by visual cortex stimulation. J Neurosci 32:3095–3100. CrossRef Medline

Kay LM, Laurent G (1999) Odor- and context-dependent modulation of mitral cell activity in behaving rats. Nat Neurosci 2:1003–1009. CrossRef Medline

Kayser C, Logothetis NK (2007) Do early sensory cortices integrate crossmodal information? Brain Struct Funct 212:121–132. CrossRef Medline

Kleemann AM, Albrecht J, Schöpf V, Haegler K, Kopietz R, Hempel JM, Linn J, Flanagin VL, Fesl G, Wiesmann M (2009) Trigeminal perception is necessary to localize odors. Physiol Behav 97:401–405. CrossRef Medline

Kollndorfer K, Kowalczyk K, Frasnelli J, Hoche E, Unger E, Mueller CA, Trattnig S, Schöpf V (2013) The chemosensory path of pain. Association for Chemoreception Sciences, Huntington Beach, CA.

Kratskin I, Hummel T, Hastings L, Doty R (2000) 3-Methylindole alters both olfactory and trigeminal nasal mucosal potentials in rats. Neuroreport 11:2195–2197. CrossRef Medline

Lakatos P, Chen CM, O'Connell MN, Mills A, Schroeder CE (2007) Neuronal oscillations and multisensory interaction in primary auditory cortex. Neuron 53:279–292. CrossRef Medline

Livermore A, Laing DG (1996) Influence of training and experience on the perception of multicomponent odor mixtures. J Exp Psychol Hum Percept Perform 22:267–277. CrossRef Medline

Lundström JN, Boesveldt S, Albrecht J (2011) Central processing of the chemical senses: an overview. ACS Chem Neurosci 2:5–16. CrossRef Medline

Luo M, Sun L, Hu J (2009) Neural detection of gases–carbon dioxide, oxygen–in vertebrates and invertebrates. Curr Opin Neurobiol 19:354–361. CrossRef Medline

Maier JX, Wachowiak M, Katz DB (2012) Chemosensory convergence on primary olfactory cortex. J Neurosci 32:17037–17047. CrossRef Medline

Paxinos G, Franklin K (2000) The mouse brain in stereotaxic coordinates, Ed 2. San Diego: Academic.

Payton CA, Wilson DA, Wesson DW (2012) Parallel odor processing by two anatomically distinct olfactory bulb target structures. PLoS One 7:e34926. CrossRef Medline

Porter J, Anand T, Johnson B, Khan RM, Sobel N (2005) Brain mechanisms for extracting spatial information from smell. Neuron 47:581–592. CrossRef Medline

Rampin O, Bellier C, Maurin Y (2012) Electrophysiological responses of rat olfactory tubercle neurons to biologically relevant odours. Eur J Neurosci 35:97–105. CrossRef Medline

Rennaker RL, Chen CF, Ruyle AM, Sloan AM, Wilson DA (2007) Spatial and temporal distribution of odorant-evoked activity in the piriform cortex. J Neurosci 27:1534–1542. CrossRef Medline

Rinberg D, Koulakov A, Gelperin A (2006) Sparse odor coding in awake behaving mice. J Neurosci 26:8857–8865. CrossRef Medline

Schaefer M, Böttger B, Silver WL, Finger TE (2002) Trigeminal collaterals in the nasal epithelium and olfactory bulb: a potential route for direct modulation of olfactory information by trigeminal stimuli. J Comp Neurol 444:221–226. CrossRef Medline

Schoenbaum G, Eichenbaum H (1995) Information coding in the rodent prefrontal cortex. I. Single-neuron activity in orbitofrontal cortex compared with that in pyriform cortex. J Neurophysiol 74:733–750. Medline

Schroeder CE, Foxe J (2005) Multisensory contributions to low-level, 'unisensory' processing. Curr Opin Neurobiol 15:454–458. CrossRef Medline

Shusterman D, Avila PC (2003) Real-time monitoring of nasal mucosal pH during carbon dioxide stimulation: implications for stimulus dynamics. Chem Senses 28:595–601. CrossRef Medline

Silver W, Finger T (1991) The trigeminal system. In: Smell and taste in health and disease (Getchell TV, Doty RI, Bartoshuk LM, Snow JB, eds), pp 97–108. New York: Raven.

Thuerauf N, Kaegler M, Dietz R, Barocka A, Kobal G (1999) Dose-dependent stereoselective activation of the trigeminal sensory system by nicotine in man. Psychopharmacology 142:236–243. CrossRef Medline

Thürauf N, Friedel I, Hummel C, Kobal G (1991) The mucosal potential elicited by noxious chemical stimuli with CO2 in rats: is it a peripheral nociceptive event? Neurosci Lett 128:297–300. CrossRef Medline

Tucker D (1971) Nonolfactory responses from the nasal cavity: Jacobson's organ and the trigeminal system. In: Handbook of sensory physiology (Beidler LM, ed), pp 151–181. Springer: New York.

Turner SL, Ray A (2009) Modification of CO2 avoidance behaviour in Drosophila by inhibitory odorants. Nature 461:277–281. CrossRef Medline

Varga AG, Wesson DW (2013) Distributed auditory sensory input within the mouse olfactory cortex. Eur J Neurosci 37:564–571. CrossRef Medline

Wang YY, Chang RB, Liman ER (2010) TRPA1 is a component of the nociceptive response to CO2. J Neurosci 30:12958–12963. CrossRef Medline

Wang YY, Chang RB, Allgood SD, Silver WL, Liman ER (2011) A TRPA1-dependent mechanism for the pungent sensation of weak acids. J Gen Physiol 137:493–505. CrossRef Medline

Wesson DW, Wilson DA (2010) Smelling sounds: olfactory-auditory sensory convergence in the olfactory tubercle. J Neurosci 30:3013–3021. CrossRef Medline

Wesson DW, Wilson DA (2011) Sniffing out the contributions of the olfactory tubercle to the sense of smell: hedonics, sensory integration, and more? Neurosci Biobehav Rev 35:655–668. CrossRef Medline

Wesson DW, Donahou TN, Johnson MO, Wachowiak M (2008) Sniffing behavior of mice during performance in odor-guided tasks. Chem Senses 33:581–596. CrossRef Medline

Wilson DA (2000) Comparison of odor receptive field plasticity in the rat olfactory bulb and anterior piriform cortex. J Neurophysiol 84:3036–3042. Medline

Wilson DA, Sullivan RM (2011) Cortical processing of odor objects. Neuron 72:506–519. CrossRef Medline

Wise PM, Wysocki CJ, Lundström JN (2012) Stimulus selection for intranasal sensory isolation: eugenol is an irritant. Chem Senses 37:509–514. CrossRef Medline

Youngentob SL, Mozell MM, Sheehe PR, Hornung DE (1987) A quantitative analysis of sniffing strategies in rats performing odor discrimination tasks. Physiol Behav 41:59–69. CrossRef Medline

Yousem DM, Williams SC, Howard RO, Andrew C, Simmons A, Allin M, Geckle RJ, Suskind D, Bullmore ET, Brammer MJ, Doty RL (1997) Functional MR imaging during odor stimulation: preliminary data. Radiology 204:833–838. Medline

Zald DH, Pardo JV (2000) Functional neuroimaging of the olfactory system in humans. Int J Psychophysiol 36:165–181. CrossRef Medline

Zelano C, Montag J, Johnson B, Khan R, Sobel N (2007) Dissociated representations of irritation and valence in human primary olfactory cortex. J Neurophysiol 97:1969–1976. CrossRef Medline